

Phonon-induced enhancement of the energy gap and critical current of superconducting aluminum films

Daniel Seligson and John Clarke

*Department of Physics, University of California, Berkeley, California 94720
and Materials and Molecular Research Division, Lawrence Berkeley Laboratory, Berkeley, California 94720*

(Received 25 July 1983)

Enhancements of the energy gap Δ and the critical current I_c have been induced in thin superconducting aluminum films near the transition temperature T_c by pulses of phonons at approximately 9 GHz. In terms of the change in temperature $|\delta T/T_c|$ necessary to produce the same enhancement in equilibrium, the gap enhancement increased smoothly with phonon power at fixed temperature and decreasing temperature at fixed phonon power; however, very close to T_c the enhancement rolled off. At relatively low phonon powers, the data were in good agreement with the theory of Eckern, Schmid, Schmutz, and Schön, but at higher power levels the data fell markedly below the predictions of the theory. The critical-current enhancements in terms of $|\delta T/T_c|$ were always larger than the gap enhancements at the same temperature and phonon power. At fixed phonon power the critical-current enhancements were nearly independent of temperature, except very close to T_c where the enhancement became small. The inclusion of the nonequilibrium quasiparticle distribution and the kinetic energy of the supercurrent in the theory relating the critical-current enhancement to the gap enhancement did not resolve the discrepancies between the two enhancements. It appears likely that there is an additional mechanism for critical-current enhancement that has not yet been identified.

I. INTRODUCTION

Wyatt *et al.*¹ and Dayem and Wiegand² discovered independently that microwave radiation could enhance the critical currents of tin microbridges. The generally accepted explanation³ of this enhancement was put forward by Eliashberg and, in more detail, by Ivlev, Lisitsyn, and Eliashberg (ILE). In their theory, photons with energies $h\nu$ less than 2Δ [where $\Delta(T)$ is the energy gap] excite quasiparticles near the gap edge to higher states, thereby freeing more states near the Fermi wave vector k_F for occupancy by pairs and enhancing the condensation amplitude. A substantial amount of experimental work ensued on the microwave enhancement of the critical current⁴⁻⁸ I_c , transition temperature^{4,6,7,9-11} T_c , energy gap,^{8,9,12-14} and order parameter¹⁵⁻¹⁷ of superconducting strips. Tredwell and Jacobsen¹⁸ observed enhancements of the Josephson-like critical current of microbridges and point contacts induced by phonon irradiation. Gray¹⁹ and Chi and Clarke²⁰ obtained gap enhancement by using tunneling experiments in which the quasiparticle distributions were modified by extraction of quasiparticles. Mooij²¹ and Pals *et al.*²² have given excellent reviews of these experiments.

Eckern, Schmid, Schmutz, and Schön²³ (ESSS) have expanded and developed the ILE theory to make it applicable not only to microwave irradiation but also to phonon irradiation and quasiparticle extraction. They also analyzed the stability of the superconducting state in the presence of these perturbations. We shall use the ESSS form of the theory extensively in the analysis of our data.

The ILE and ESSS theories involve two crucial assumptions, first, that the phonons remain in thermal equilibrium, and, second, that the quasiparticles have an energy-independent recombination rate. Neither of these assumptions were necessary in the work of Chang and Scalapino²⁴ who solved the kinetic equations for microwave stimulation and showed that for typical experimental conditions the electrons and phonons are in marked disequilibrium, to an extent that increases as the phonon trapping time increases. They also showed that the increase of the quasiparticle recombination rate with increasing energy leads to a net decrease of the number of quasiparticles, and that this reduction is as significant in the gap enhancement as the removal of the low-lying pair-blocking quasiparticles. This method has been applied to the case of phonon stimulation by Cirillo *et al.*²⁵ More recently, Lesieur and Perrin²⁶ used a two-temperature model as an approximation to the solution of the kinetic equations, and found similar results to those of Chang and Scalapino²⁴ for the case of microwave-induced gap enhancement.

Although there now seems to be general agreement that superconductivity can be enhanced by a suitable perturbation, some anomalies remain unresolved. For example, Dahlberg *et al.*⁸ observed that microwave-induced critical-current enhancement was not necessarily accompanied by gap enhancement. Similarly, van Attekum and co-workers^{16,17} found that the order parameter enhancement was about one-half that expected from the observed critical-current enhancement. A number of explanations^{14,17,27-29} have been put forward to account for these discrepancies, but none of them can account satisfactorily

for the lack of gap enhancement observed by Dahlberg *et al.*

A possible explanation for the discrepancy between gap and critical-current enhancements is the nonuniformity of the microwave fields over the surface of the superconducting film.¹⁴ Partly for this reason, we decided to study the gap and critical-current enhancements in aluminum films due to phonon irradiation. In the experimental configuration used, the phonon intensity is expected to be uniform over the superconductor. The main objectives were first, to examine whether the discrepancies between the gap and critical-current enhancements existed in the case of the phonons, and second, to compare the enhancements with theoretical predictions as quantitatively as possible. Section II summarizes the relevant theory, Sec. III describes the experimental techniques, while Sec. IV presents the results and compares them with the theory. Section V contains a concluding summary.

II. THEORY

We briefly review the ILE theory³ of phonon-induced gap enhancement, as described by ESSS.²³ One introduces into the Boltzmann equation for the quasiparticles a drive term \dot{n}_D that describes the time rate of change of occupancy of a state with energy E in the presence of phonons of frequency ν . Using the relaxation time approximation, one can relate \dot{n}_D to the steady-state occupancy, $n(E)$:

$$\dot{n}_D = [n(E) - n_T(E)]/\tau_E. \quad (2.1)$$

Here, $n_T(E)$ is the Fermi function, and τ_E^{-1} is the inelastic scattering rate at $E=0$ and $T=T_c$. Because τ_E^{-1} is energy and temperature dependent, the use of Eq. (2.1) restricts the theory to the range $\Delta \ll k_B T_c$. It is also assumed that the phonons are in thermal equilibrium at the bath temperature T . With these restrictions, and with the further assumptions that $h\nu \ll k_B T_c$ and that the departure from thermal equilibrium, $n - n_T$, is small, ESSS find

$$n - n_T = \dot{n}_D \tau_E = B \left[N_1(E - h\nu) \left[1 - \frac{\Delta^2}{E(E - h\nu)} \right] - N_1(E + h\nu) \left[1 - \frac{\Delta^2}{E(E + h\nu)} \right] \right], \quad (2.2)$$

where

$$B = N_R \tau_E / 8N(0)k_B T_c, \quad (2.3)$$

$N(0)$ is the single spin density of states at the Fermi level, $N_1(E) = [E/(E^2 - \Delta^2)^{1/2}] \Theta(E - \Delta)$ is the BCS density of states, and N_R is the number of quanta absorbed per unit volume and unit time in the normal state. If $2\Delta < h\nu$, an additional term is present in \dot{n}_D that dramatically increases the quasiparticle density and thereby destroys the superconducting state.¹⁸ This is in contrast to the case of microwave radiation, where the different coherence factors lead to less severe pair breaking, and permit T_c enhancement.^{6,7,9-11}

One inserts $n(E)$ into the BCS integral equation for the gap to obtain the nonequilibrium value of Δ . Since we are interested only in temperatures close to T_c , we can express the integral in the Ginzburg-Landau (GL) form:

$$\Delta [(T - T_c)/T_c + \beta(\Delta/k_B T_c)^2 - \chi] = 0, \quad (2.4)$$

where $\beta = 7\zeta(3)/8\pi^2 \approx 0.1066$, and

$$\chi = - \int dE (n - n_T)/(E^2 - \Delta^2)^{1/2} \quad (2.5)$$

is the "gap control." Near T_c , χ represents either an increase in the transition temperature by an amount χT_c or a decrease in the temperature of the electrons by the same amount. ESSS show that χ is proportional to B , and functionally dependent only on the ratio $\Delta/h\nu \equiv u$. Thus Eq. (2.4) can be reduced to the form

$$u [(T - T_c)/T_c + \beta(h\nu/k_B T_c)^2 u^2 - BG(u)] = 0, \quad (2.6)$$

where $G(u)$ is a specified function.²³ Equation (2.6) can be solved numerically or graphically for Δ at a given phonon frequency and intensity.

In the region of experimental interest in which the term $h\nu/k_B T_c$ may not be small, ESSS (in their Appendix F) show that an additional term arises that can be regarded as an increase in the temperature of the electrons relative to that of the phonons:

$$\chi_0 = -0.68(h\nu/k_B T_c)B. \quad (2.7)$$

In addition, as pointed out by Mooij,²¹ there is a second heating effect that must be taken into account. The temperature T in Eqs. (2.4) and (2.6) refers to the phonon distribution in the superconducting film, and this temperature is higher than the temperature of the helium bath because of the nonzero Kapitza resistance between the sample and its surroundings. The incident phonon power absorbed at T_c is $N_R h\nu A d$, where A is the surface area of the film and d is its thickness. Below T_c the absorbed power decreases by the factor³⁰ $2/[1 + \exp(\Delta/k_B T)]$, but we will not include this temperature dependence (see below). If we assume that all of the absorbed energy is thermalized, the increase in temperature of the film is $N_R h\nu d R_K$, where R_K is the Kapitza resistance governing heat flow through both surfaces. Since experimentally we can determine only the temperatures of the electrons and of the bath, it is convenient to combine both heating terms into one:

$$\begin{aligned} \chi_H &= \chi_0 - 8N(0)(k_B T_c)(k_B R_K)(Bd)(h\nu/k_B T_c)/\tau_E \\ &= -BHh\nu/k_B T_c. \end{aligned} \quad (2.8)$$

Combining Eqs. (2.6) and (2.8), we obtain

$$u \{ (T - T_c)/T_c + \beta(h\nu/k_B T_c)^2 u^2 - [G(u) - (h\nu/k_B T_c)H]B \} = 0, \quad (2.9)$$

where from now on T is interpreted as the bath temperature. Thus to observe enhancement it is essential that $G(u) > (h\nu/k_B T_c)H$. Since $G(u) \leq 2.64$, there is a maximum value of H for which enhancement can be observed for a given value of $h\nu/k_B T_c$.

It should be emphasized that Eq. (2.9) omits two effects, both of which were calculated by Chang and Scalapino.²⁴ First, the ILE theory assumes that the phonons are always in thermal equilibrium, whereas in fact they are not. Second, the use of a relaxation-time approximation implies that the increase of the quasiparticle recombination rate with energy is neglected, and that the enhancement due to a reduction in quasiparticle density is therefore omitted. One may hope that both effects are small in the limit $\Delta \ll k_B T_c$. In practice, of course, one is interested in the magnitude of the enhancements at temperatures where $\Delta/k_B T_c$ is not small. In this range, the validity of the ILE theory is uncertain. In addition to the two effects just described, the terms τ_E , R_K , N_R , H , and B are all strongly temperature dependent, but there seems little point in imposing these dependences on a theory that is in any case valid only for small $\Delta/k_B T_c$. Thus we shall fit the theory to the data near T_c , rather than over an extended temperature range.

We now turn to a consideration of the critical-current measurements. If the cross section of the sample is small compared with λ^2 , where $\lambda(T)$ is the penetration depth, the supercurrent density j_s is uniform. In thermal equilibrium, the kinetic energy of the supercurrent introduces a term³⁰

$$(4/27\beta^2)(j_s/j_{c0})^2(\Delta/k_B T_c)^{-4} \quad (2.10)$$

into the GL equation. To find the critical current $j_c(T)$, one solves the GL equation for the maximum value of j_s to find^{6,30}

$$j_c(T) = j_{c0}(1 - T/T_c)^{3/2}, \quad (2.11)$$

where

$$j_{c0} = 1.55[H_c(0)/\lambda_L(0)](l/\xi_0)^{1/2}. \quad (2.12)$$

Here, $H_c(0)$ and $\lambda_L(0)$ are the critical field and London penetration depth at zero temperature, l is the electronic mean free path, and $\xi_0 = \hbar v_F / \pi \Delta(0)$, where v_F is the Fermi velocity. In the present experiments, the thickness d of the films is typically less than $2\lambda(T)$, but the width w is substantially greater than λ , so that the criterion $wd < \lambda^2$ is not satisfied. Skocpol³¹ has studied this situation in detail for tin microbridges, and has found reasonable agreement between experimentally determined critical currents and calculations that take into account the nonuniform current flow. From these measurements and calculations, for our own samples in the range $T \geq 0.95T_c$ we expect the deviations from the predictions of Eq. (2.11) to be no greater than the uncertainty in the determination of the sample properties.

In most previous work, the critical-current enhancements have been compared with the theory (which calculates gap enhancement) by assuming that j_c/Δ^3 has the same value as in thermal equilibrium, and inferring the gap enhancement from the measured gap enhancement. In fact, as shown by Weiss²⁷ and Entin-Wohlman,²⁸ when the dependence of the supercurrent on the quasiparticle distribution function and the kinetic energy of the supercurrent are included in the nonequilibrium GL equation

one finds that j_c/Δ^3 is an increasing function of the microwave or phonon intensity. A discussion of these effects will be deferred until Sec. IV D.

In concluding this section, we note that for a given phonon intensity the parameter B scales as $\tau_E/\hbar k_B T_c$. Given that we wish to work in the liquid-⁴He temperature range, this fact immediately leads us to choose Al as the superconductor to study experimentally. Values of the relevant parameters for Al are listed in Table I.

III. EXPERIMENTAL TECHNIQUES

A. Phonon generation

The phonons were generated by the piezoelectric transduction of a microwave pulse, following the method of Tredwell and Jacobsen¹⁸ (see Fig. 1). A klystron that generated up to 100 mW of continuous microwave power and could be tuned between 8 and 12 GHz was coupled to a traveling-wave tube (TWT) amplifier that produced 1-kW pulses, typically with a duration of 1 μ sec and a repetition rate of 50 Hz. The signal was monitored with a diode detector, and coupled via a waveguide into a screened room containing the cryostat. A directional coupler tapped off -20 dB of the power reflected from the insert. Just above the top of the cryostat the waveguide was vacuum sealed with an infrared filter. The stainless-steel waveguide inside the cryostat was evacuated, the lower end being closed with a Mylar seal just above the copper cavity which contains superfluid liquid helium. The transducer was an X-cut single crystal of quartz 25 mm long and 4 mm in diameter. The end faces were polished flat to 50 nm and cut parallel to within 4" of arc. The crystal was mounted horizontally in the cavity, the inner end facing a tuning plunger to form a reentrant cavity the resonant frequency of which could be tuned from 8 to 11 GHz.

B. Sample fabrication

Samples were fabricated from Al films typically 100 nm thick on one end of a quartz crystal in one of the two configurations, W (wide junction) and N (narrow junction) shown in Fig. 2. In each case we measured the critical current of a strip of Al about 300 μ m long and 3–10 μ m wide with $T_c \approx 1.25$ K and $l \approx 45$ nm. To measure the energy gap we fabricated a tunneling contact to an Al film doped with oxygen to give a transition temperature of about 1.8 K. The phonon-induced enhancement of this film was substantially reduced compared to that of the clean film for two reasons: First, we expect N_R to scale with the normal-state ultrasonic attenuation, which in turn is proportional to l (Ref. 39); since l was reduced by a factor of 20–50 in the dirty films relative to the clean films, N_R was reduced by the same factor. Second, at the usual temperature of the experiment, close to T_c of the clean film, the reduced temperature of the dirty film was about 0.6 so that $G(\Delta/h\nu)$ was an order of magnitude smaller than the value expected in the clean film. To check the dependence of the enhancement on l , we mea-

TABLE I. Parameters for aluminum.

Free electron density, ^a N	$1.81 \times 10^{29} \text{ m}^{-3}$
Single spin density of states, ^b $N(0)$	$1.74 \times 10^{28} \text{ eV}^{-1} \text{ m}^{-3}$
Fermi velocity, ^c v_F	$1.36 \times 10^6 \text{ m sec}^{-1}$
Coherence length ^d ($T_c = 1.19 \text{ K}$), $\xi_0 \equiv \hbar v_F / \pi \Delta(0)$	$1.6 \mu\text{m}$
London penetration depth, ^d ($T_c = 1.19 \text{ K}$) $\lambda_L(0)$	16 nm
Critical field, ^e $H_c(0)$	$8 \times 10^3 \text{ A m}^{-1}$
Longitudinal speed of sound, ^f c_l	$6.65 \times 10^3 \text{ m sec}^{-1}$
Transverse speed of sound, ^f c_t	$3.26 \times 10^3 \text{ m sec}^{-1}$
Resistivity—mean free path product, ^g ρl	$9 \times 10^{-16} \Omega \text{ m}^2$
Transition temperature, ^h T_c	$1.23\text{--}1.30 \text{ K}$
Inelastic scattering time, ⁱ τ_E	12 nsec
Mean free path, ^h l	45 nm

^aReference 32.^bReference 33.^cReference 34.^dReference 35.^eReference 6.^fReference 36.^gReference 37.^hRepresentative values for films used in this study.ⁱReference 38.

sured the critical-current enhancement in a dirty film at $T/T_c = 0.98$, and found it to be a factor of 30 less than that in a clean film at the same reduced temperature and phonon power. The implied relative constancy of the energy gap of the dirty film in the presence of the phonons greatly facilitated the determination of the gap enhancement of the clean films from the tunneling measurements. Furthermore, the lack of gap anisotropy in the dirty films sharpened the gap structure in the current-voltage (I - V) characteristics.

To make samples in the configuration of Fig. 2(a), type W , we first deposited (in 10^{-4} Torr of oxygen) a doped Al

film about $800 \mu\text{m}$ wide, and then evaporated SiO to mask off the edges and leave a window approximately $300 \times 300 \mu\text{m}^2$. Oxygen was admitted to the bell jar to oxidize the film. After pumping out the oxygen, we deposited a relatively clean Al film to complete the junction. Typical tunneling resistances were $0.1\text{--}20 \Omega$. Finally, using standard photolithographic procedures, we etched out a narrow strip in the clean film for the critical-current measurements. We also fabricated some junctions with the order of the clean and dirty Al films interchanged to investigate the possible effects due to different phonon coupling or different Kapitza resistances to the substrate and helium bath, but no systematic differences between the two configurations could be detected. The type- N samples were fabricated in a very similar way to type W with the dirty Al deposited first. This configuration has the obvious advantage that one measures the enhancements in Δ and I_c in exactly the same sample. In this case, the tunnel junction has resistances in the range $4\text{--}10 \Omega$. Our experimen-

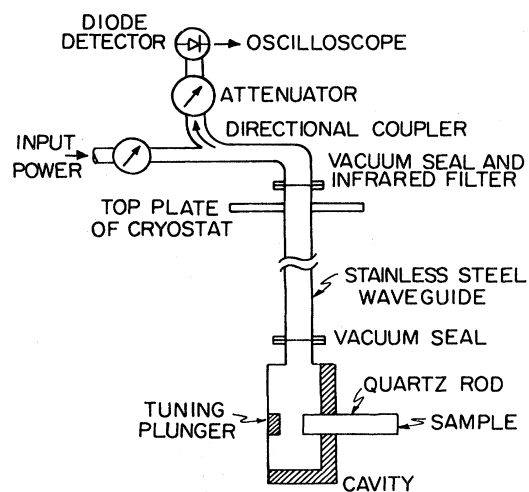


FIG. 1. Quartz crystal, microwave cavity, and waveguides for input and reflected microwaves.

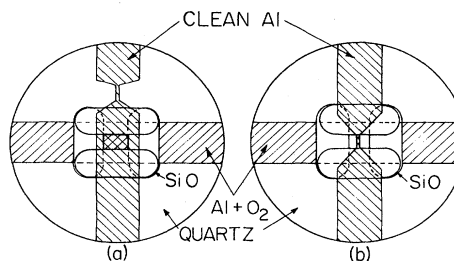


FIG. 2. Sample configurations: (a) type W , wide junction with microstrip to one side; (b) type N , narrow junction with microstrip forming the upper electrode of the junction.

tal configuration is expected to give a rather uniform phonon irradiation across the whole sample, as compared with the microwave case in which there may be a tendency for the microwave currents to concentrate near the edges of the film.

Indium- and solder-coated copper wires were attached to the samples with small indium pads to enable us to make four-terminal I - V measurements of both the junction and the narrow strip. The quartz rod was inserted into the cavity, positioned to give an appropriate resonant frequency, clamped with a spring clip, and sealed into place with silver paint.

C. Measurement techniques

The equilibrium energy gap $\Delta(T)$ of the clean Al film was determined by plotting the I - V characteristics on an X - Y recorder, and obtaining measurements of the sum and difference of the two gaps. The circuit for measuring the enhanced values of Δ is shown in Fig. 3. The junction was biased with a constant current. Any pulsed voltage change across the junction was amplified, monitored with an oscilloscope, and measured with a boxcar integrator. Because the microwave pulse immediately drove the films into the normal state, the very large voltage pulse that ensued was blanked out by means of a field-effect transistor switch. By the time the phonons reached the sample, 4.2 μ sec later, the sample had recovered from the electromagnetic pulse, and the voltage pulse due to the modification of the I - V characteristic by the phonons could be measured. The integrated output of the boxcar was measured with a voltmeter, and also added to the equilibrium voltage across the junction by means of a summing amplifier to produce a reconstruction of the total voltage. A low-pass filter in the voltage amplifier together with the very low duty factor of the pulses ensured that the presence of the pulses had a negligible effect on the measurement of the equilibrium voltage. By slowly sweeping the bias current we could obtain the nonequilibrium I - V characteristic and hence the gap enhancement. Alternatively, we could determine the gap enhancement by biasing the junction at the sum of the gaps and noting the magnitude of the voltage pulse, which arose entirely from the change in the energy gap of the clean film because the O_2 -doped

film was unaffected by the phonons. The system was calibrated by applying voltage pulses of known amplitude to the input.

Only a small fraction of the incident phonon power was absorbed by the Al films,⁴⁰ the rest of it being reflected at the Al/He interface. After reflection at the other end of the crystal, the phonons were again incident on the films, inducing another voltage pulse. The system noise was sufficiently low and the quartz crystal was sufficiently accurately cut that as many as 17 of these echoes have been observed.

The equilibrium values of the critical current of the strip were measured from the I - V characteristics displayed on an oscilloscope. The enhanced values in the presence of the phonon pulse were measured by applying a rectangular pulse of current that was turned on and off during the phonon pulse. The voltage across the strip was monitored on an oscilloscope, and the amplitude of the current pulse was increased until the onset of voltage was detected. The amplitude of the pulse, measured with the boxcar integrator, was taken as the critical current. The values were averaged for positive- and negative-going current pulses; the difference between the two polarities was usually less than 5%. The calibration was checked frequently during a series of measurements by comparing the equilibrium value of the critical current obtained with the pulsed method with that obtained from the low-frequency I - V measurements.

The temperature of the helium bath could be lowered to about 1.05 K, and was regulated by means of a carbon resistance thermometer in a bridge circuit the output of which supplied current to a heater in the bath. Stringent precautions were taken to ensure that the microwaves did not affect the thermometry. The thermometer was enclosed in a copper mesh to shield it from the microwave field. We used the I - V characteristic of a junction to test the efficiency of this shielding. We regulated the helium bath at some fixed temperature, and detuned the cavity so that no phonons were generated by the microwaves. We then determined that the gap structure in the presence of pulsed or continuous microwaves at the maximum available power was indistinguishable from the structure in the absence of microwaves.

IV. RESULTS AND COMPARISON WITH THEORY

A. Equilibrium measurements

The temperature dependence of $\Delta(T)$ determined from the tunnel junctions was always within 2% of the BCS value. The temperature dependence of $I_c(T)$ was in good agreement with the prediction of Eq. (2.11) above $0.95T_c$. The magnitude of the critical current was within 30% of the value predicted using the sample dimensions and the values of $H_c(0)$, $\lambda_L(0)$, ξ_0 , and ρl (ρ is the resistivity) listed in Table I. Good agreement between the measured and predicted magnitudes provides strong evidence that the critical current of the strip was determined by the macroscopic dimensions of the sample, rather than by an anomalously narrow region. Furthermore, the values of

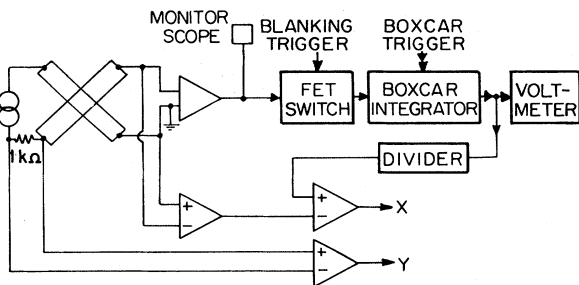


FIG. 3. Block diagram of electronics for measuring gap enhancement.

T_c obtained by extrapolating Δ and $j_c^{2/3}$ to zero were the same to within a few milliKelvin, and the width of the resistive transition, measured with a very small current, was typically 5 mK. These observations suggest strongly that phase slip centers were not present.

B. Gap and critical-current enhancement: general features

A representative reconstruction of the I - V characteristic of a small-area tunnel junction is shown in Fig. 4. The sharp rise in current at the sum of the gaps is moved to a higher voltage in the presence of the phonons, indicating gap enhancement. We note that one cannot determine accurately the nonequilibrium value of the cusp at the difference of the energy gaps because of hysteretic switching (induced by the pulsed TWT) to the sum of the gaps that occurs at voltages below the cusp. It is for this reason that we must determine the enhancement from the change in the sum of the gaps.

The inset of Fig. 4 is an expanded region of the I - V characteristic of another junction, showing a pronounced feature in the quasiparticle current at a voltage $h\nu/e \approx 35 \mu\text{V}$ below the cusp at the difference of the energy gaps. This effect,^{24,25,41} first seen in microwave enhancement experiments by Horstman *et al.*⁴² occurs because the absorbed phonons reduce the quasiparticle density for $E < \Delta + h\nu$, but increase the density sharply for $E \geq \Delta + h\nu$. In some of the small-area junctions, there was considerable structure due to phonon-assisted tunneling⁴³ at the higher power levels, as illustrated in Fig. 5. The position of the current risers, at $(\Delta_1 + \Delta_2) \pm n h\nu$ (n is an integer), provided a useful confirmation of the calibration of the system. The step about $25 \mu\text{V}$ below the sum of the gaps in Fig. 4 appears to be at the incorrect voltage to arise from phonon-assisted tunneling. We suspect, however, that this anomaly may arise because the voltage

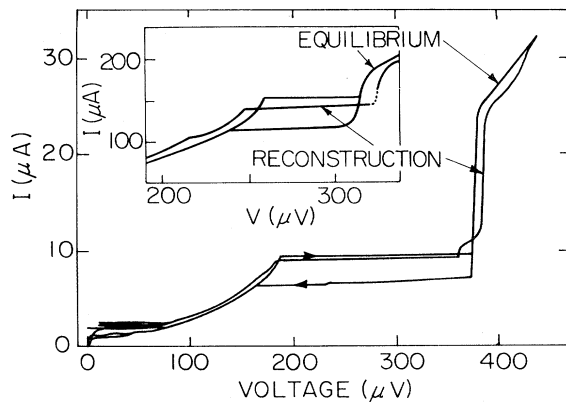


FIG. 4. Reconstructed I - V characteristic of junction $N4$ in the presence of phonons ($T/T_c=0.908$, $h\nu/k_B T_c=0.341$, $B=0.10$). Equilibrium characteristic is also shown. Inset is I - V characteristic of junction $W2$ ($T/T_c=0.993$, $h\nu/k_B T_c=0.333$, $B=12.0 \times 10^{-3}$) showing a cusp in the quasiparticle current at a voltage $h\nu/e \approx 35 \mu\text{V}$ below the difference of the energy gaps.

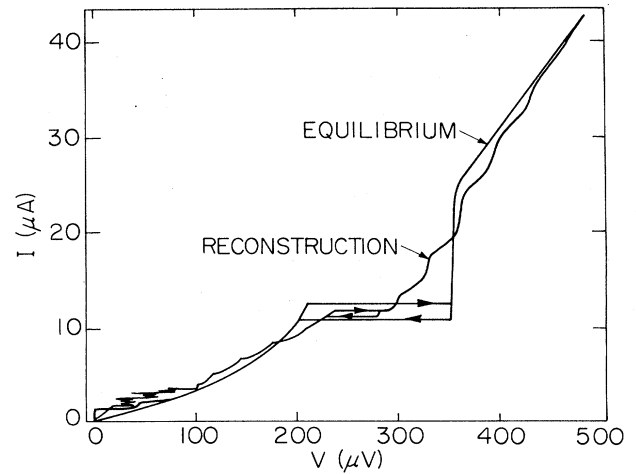


FIG. 5. Reconstructed I - V characteristic of junction $N2$ showing both gap enhancement and phonon-assisted tunneling ($T/T_c=0.950$, $h\nu/k_B T_c=0.337$, $B=0.10$). Equilibrium characteristic is also shown.

switched from the cusp to the upper portion of a rather broad step. Although we cannot completely rule out the possibility that this feature represents a second gap induced by the phonons,²³ we have no convincing evidence for such behavior in this or any other junction that we studied.

We now turn to a description of the gap and critical-current enhancement as a function of temperature and phonon intensity. Figures 6(a) and 6(b) show the gap and critical current versus temperature for a narrow sample for six levels of phonon power; the equilibrium values are also plotted. The temperature dependence of the equilibrium gap is in excellent agreement with the BCS prediction, while the temperature dependence of the critical current follows the Ginzburg-Landau prediction for temperatures above about $0.95T_c$. At a fixed temperature, both the gap and critical current increase smoothly as the phonon power is increased. It is also evident that the critical current is increased relatively more than the gap at a given temperature and phonon power. We never observed systematic differences between the critical-current enhancements observed in the two different types of samples.

To facilitate comparison of the two enhancements, it is convenient to represent each of them in terms of the change in reduced temperature, $\delta T/T_c$, that in equilibrium would result in the same increment in gap or critical current. This procedure is shown inset in Fig. 6(a) for the gap enhancement. In both cases, we used the measured (rather than the theoretical) equilibrium curves to obtain $\delta T/T_c$. In the case of gap enhancement, we can compare experimentally determined values of $-\delta T/T_c$ directly with the theoretical expression $(\chi + \chi_H)$. A discussion of the theory of critical current enhancement will be deferred until Sec. IV D. Figure 7 shows the gap and critical-current enhancements in terms of $\delta T/T_c$ for the narrow sample of Fig. 6 and for a wide sample. We note that the

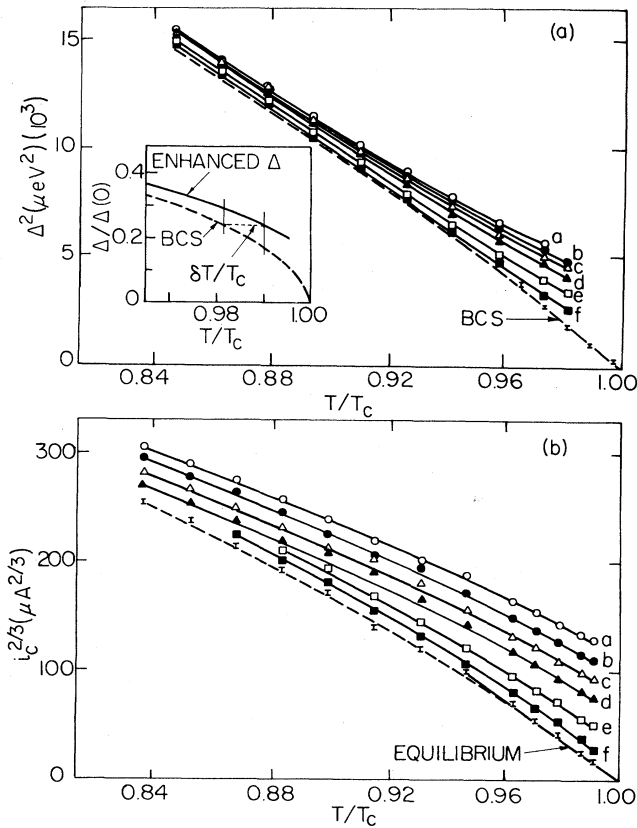


FIG. 6. (a) Gap and (b) critical current vs T/T_c for sample N1 [$h\nu/k_B T_c = 0.328$, $B(0 \text{ dB}) = 0.22$] for the following power levels: a, 0 dB; b, -2 dB; c, -4 dB; d, -6 dB; e, -10 dB; f, -15 dB. Curves are drawn to guide the eye. Points with error bars are measured in equilibrium; dashed lines are BCS prediction. Inset shows relationship between enhanced gap and $\delta T/T_c$.

curves for gap and critical-current enhancement are qualitatively rather different. Over most of the temperature range, at constant phonon power $\delta T/T_c$ falls steadily as the temperature is lowered in the case of the gap, but remains roughly constant in the case of the critical current. However, for the wide sample, at constant phonon power $\delta T/T_c$ decreases in both cases as the temperature is raised above about $0.99T_c$. A similar feature was seen in all the samples we studied, although the temperature at which the rolloff began varied from about $0.99T_c$ to about $0.995T_c$. We note that the temperature at which pair breaking [$h\nu \geq 2\Delta(T)$] occurs is about $0.996T_c$ for 10-GHz phonons. Thus the rolloff in the enhancement began at values of $2\Delta(T)/h\nu$ significantly greater than unity. As expected theoretically, we never observed enhancement of T_c in either type of measurement. The gap and critical-current enhancements also differ quantitatively in that the critical-current enhancement is always substantially larger than the gap enhancement. Thus, for the narrow sample, the critical-current enhancement at the

highest phonon power exceeds the maximum gap enhancement at the same power by a factor of about 2; for the wide sample, the corresponding factor is about 5.

Finally, we note that, at the available phonon power levels, we never observed a saturation and a subsequent decrease in the enhancement of either Δ or I_c as the phonon power was increased at constant sample temperature.

C. Fit of gap enhancement to theory

To fit the data to Eq. (2.9) we have to determine two parameters: B , which is a measure of the phonon intensity, and H , which is a measure of the increase of the electron temperature relative to the bath temperature. Preliminary attempts to fit the data indicated that the theory failed at the higher phonon power levels; thus we fitted the data at lower levels. A representative fit is illustrated in Fig. 8, in which the data were fitted at -10 dB. The values of the fitting parameters (Table II) were $B = (1.4 \pm 0.1) \times 10^{-3}$ and $H = 1.6 \pm 0.2$. The theory was fitted to the data at temperatures above $0.95T_c$, and the uncertainties express the variations in B and H (B and H are dimensionless) that could be made without introducing a disagreement between theory and experiment of more than $\pm 10\%$. We see that the theory fits the data reasonably well over most of the temperature range, but fails to predict the rolloff in the data above about $0.99T_c$. The four sets of data taken at lower power levels are also well fitted with the same value of H and appropriately scaled values of B , although the theory again fails to predict the high-temperature rolloff in the data. On the other hand, the data set (a) at a power level 3 dB above the set (b) fall below the theory over most of the temperature range. Data taken at higher power levels (not shown) are in even greater disagreement with the theory. These discrepancies are illustrated in Fig. 9 where we have plotted $\delta T/T_c$ versus relative power at $T/T_c = 0.99$. As the relative phonon power level is increased above about -10 dB, theory and experiment diverge rapidly.

At a phonon power level of -10 dB, our fitted value of B is 1.4×10^{-3} . Thus from Fig. 9 it appears that the theory fails to fit the data for this sample for values of B above about 2×10^{-3} . The curvature in the data is reminiscent of the calculations of Chang and Scalapino²⁴ for microwaves and Cirillo *et al.*²⁵ for phonons when phonon trapping effects are taken into account, leading us to wonder whether the present theory fails at the higher power levels due to the neglect of the nonequilibrium phonon distribution. It is thus of some interest to estimate the value of τ_{es}/τ_B , the ratio of the phonon escape time and the pair breaking time. To do so, we must estimate R_K .

From the fitted value of H and Eq. (2.8) we find R_K (for both sides of the Al film) to be $5.0 \times 10^{-4} \text{ K m}^2 \text{ W}^{-1}$, and we first compare this value with other estimates.^{44,46} It is difficult to determine the value expected for the Al/He interface: A reasonable choice⁴⁷ at 1.25 K might be $10^{-3} \text{ K m}^2 \text{ W}^{-1}$. Thus the contribution of the Al-SiO₂ interface in our experiments is also roughly $10^{-3} \text{ K m}^2 \text{ W}^{-1}$. This value is about a factor of 3 greater than

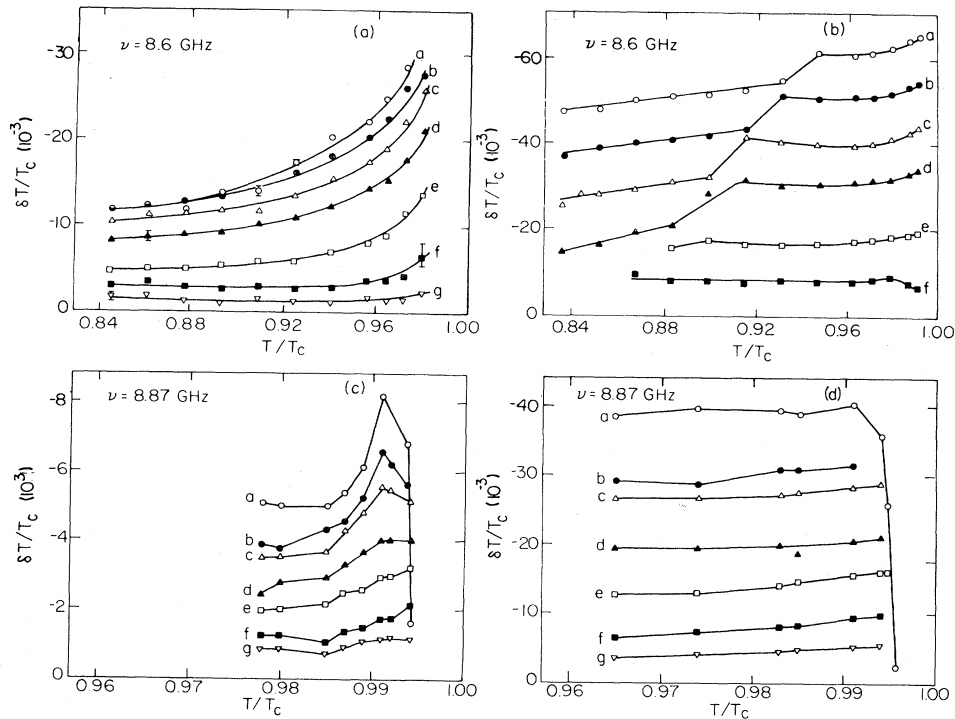


FIG. 7. (a) and (b) show $\delta T/T_c$ for gap and critical-current enhancements vs T/T_c from the data set in Fig. 6; (c) and (d) show $\delta T/T_c$ for gap and critical-current enhancements vs T/T_c for sample *W2* [$h\nu/k_B T_c = 0.333$, $B(0 \text{ dB}) = 0.012$] for the following power levels; a, 0 dB; b, -2 dB; c, -3 dB; d, -5 dB; e, -7 dB; f, -10 dB; g, -13 dB; h, -17 dB; i, -20 dB. Lines are drawn to guide the eye.

the value of $3.7 \times 10^{-4} \text{ K m}^2 \text{ W}^{-1}$ at $T = 1.25 \text{ K}$ given by Cheeke *et al.*⁴⁹ Since the value of R_K depends strongly on the procedures for substrate cleaning,^{48,50} we feel that this discrepancy is not unacceptable. Given R_K , we can esti-

mate the mean transmission coefficient $\bar{\eta}$ for phonons in the aluminum from the expression given by Anderson⁴⁵

$$\bar{\eta} = 30\hbar^3 / \pi^2 k_B^4 R_K T^3 (c_l^{-2} + 2c_t^{-2}). \quad (4.1)$$

Here, $\bar{\eta}$ is the transmission coefficient averaged over angle and over the three modes of propagation, and c_l and c_t are the longitudinal and transverse sound velocities. At $T = 1.25 \text{ K}$ with the values of c_l and c_t from Table I we find $\bar{\eta} = 2.4 \times 10^{-4} / R_K$. Thus, for $R_K = 5.0 \times 10^{-4} \text{ K m}^2 \text{ W}^{-1}$, we obtain $\eta \approx 0.5$. The escape time for phonons,³⁶

$$\tau_{\text{es}} = 4d / \bar{\eta} \bar{c}_s, \quad (4.2)$$

is thus about 2×10^{-10} sec, where we have taken $d = 100 \text{ nm}$ and an average sound velocity \bar{c}_s of $4.4 \times 10^3 \text{ msec}^{-1}$. We can estimate the pair breaking rate τ_B^{-1} from Kaplan *et al.*⁵¹ Above $0.85 T_c$, assuming a typical phonon energy of $2\Delta(T)$, we find $\tau_B \gtrsim 3\tau_0^{\text{ph}} \approx 7 \times 10^{-10}$ sec, where $\tau_0^{\text{ph}} = 2.4 \times 10^{-10}$ sec is the characteristic phonon scattering time in Al. Thus we find $\tau_{\text{es}} / \tau_B \lesssim 0.3$ for this particular sample. An inspection of the results of Chang and Scalapino²⁴ and Cirillo *et al.*²⁵ reveals that phonon trapping has significant effects on the gap enhancement only for $\tau_{\text{es}} / \tau_B > 2$. For the much smaller value of $\tau_{\text{es}} / \tau_B$ obtained from the experiment, phonon trapping and the effects of the nonequilibrium phonon distribution probably play a rather minor role, and are unlikely to account for the discrepancy between the data and the ESSS theory.

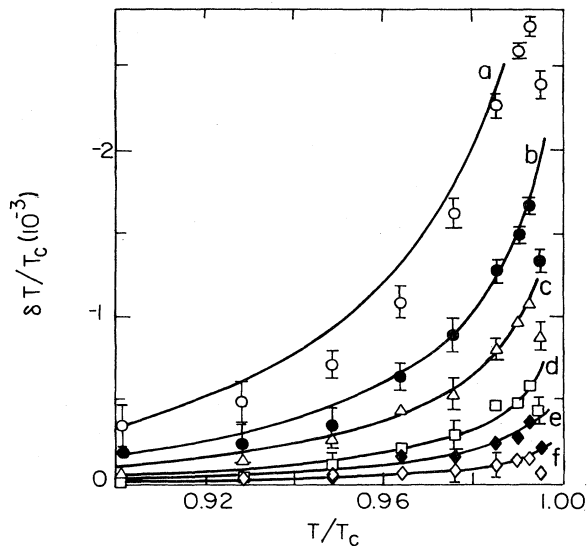


FIG. 8. Gap enhancement $\delta T/T_c$ vs T/T_c for sample *W4* ($h\nu/k_B T_c = 0.333$). Lines represent predictions of Eq. (2.7), fitted at -10-dB power level. Power levels: a, -7 dB; b, -10 dB; c, -12 dB; d, -17 dB; e, -20 dB.

TABLE II. Parameters for gap enhancement in nine samples.

Sample	T_c (K)	d (nm)	ν (GHz)	$\frac{h\nu}{k_B T_c}$	Power at fit (dB)	B (10^{-3})	H	$R_K(T_c)$ ($10^{-4} \text{ K m}^2 \text{ W}^{-1}$)	$B(0, \text{dB})$ (10^{-3})	$\delta T/T_c^c$ (10^{-3})
$W1^a$	1.310	200	9.01	0.328	-9	5.6 ± 1.0	1.2 ± 0.5	1.5 ± 1.5	44	-7.5
$W2^a$	1.274	210	8.87	0.333	-5	3.8 ± 0.6	1.6 ± 0.4	2.5 ± 1.1	12	-8
$W3^b$	1.330	100	8.83	0.317	-10	1.3 ± 0.2	1.4 ± 0.3	3.8 ± 1.7	13	-6
$W4$	1.330	100	9.26	0.333	-10	1.4 ± 0.1	1.6 ± 0.2	5.0 ± 1.2	14	-4
$W5$	1.261	100	8.88	0.337	-6	1.6 ± 0.3	5.3 ± 0.35	5.2 ± 2.0	21	-7
$W7$	1.212	185	8.43	0.333	-10	16.4 ± 1.5	2.0 ± 0.3	4.2 ± 0.9	164	-17
$N1$	1.264	100	8.60	0.328	-10	21.6 ± 2.0	1.65 ± 0.2	5.6 ± 1.0	216	-29
			9.66	0.368	-4	11.0 ± 1.2	2.0 ± 0.3	7.6 ± 1.5	27.5	-14
$N2$	1.252	100	8.81	0.337	-6	11.5 ± 2.0	1.2 ± 0.4	2.9 ± 2.3	46	-15
$N4$	1.234	100	8.81	0.341	-10	11.2 ± 1.4	1.25 ± 0.35	3.4 ± 2.0	112	-26
			9.94	0.386	-5	22.8 ± 3.1	1.65 ± 0.3	5.5 ± 1.7	72	-29

^aFilm is base electrode; in all other samples, film is counter electrode.

^bTransverse phonons.

^c0 dB, $0.98T_c$.

It is of interest to consider the value of τ_{es}/τ_B above which no gap enhancement would be observed at any phonon power. Since we require $H < G(\Delta/h\nu)(h\nu/k_B T_c)^{-1}$ for enhancement (see Sec. II), using the maximum value of $G(\frac{1}{2})=2.64$ and Eqs. (2.8), (4.1), and (4.2) we find an upper limit on τ_{es}/τ_B of 2.4.

The data presented for sample $W4$ are representative of all the large area junctions investigated. The essential parameters for five other large-area junctions are listed in Table II: T_c , d , ν , $h\nu/k_B T_c$, the power at which the data were fitted, the fitted values of B and H , the derived value of R_K , the value of B at 0 dB scaled from the value at the

fitted power, and, finally, the value of $\delta T/T_c$ observed at 0 dB at $T/T_c=0.98$. We note that the values of B at which the data were fitted were sometimes substantially higher than for $W4$; however, the theory predicted the observed power dependence correctly for values up to the value listed. In general, we fitted the data at temperatures above $0.95T_c$. The rather large error bars associated with some of the results usually reflect a scarcity of data in this temperature range. We note that in $W1$ and $W2$ the film under investigation was the base electrode rather than the counter electrode used in all of the other samples. The value of R_K obtained for $W1$ is unphysically low, giving rise to $\eta > 1$; however, the uncertainty in R_K is so large that this result should not be taken seriously. For sample $W3$ we used transverse phonons, obtaining values of B and H that are not out of the range of the values of the other samples for which we used longitudinal phonons.

The results for three narrow junctions are also presented in Table II. There was a qualitative difference between the wide and narrow junctions in that $\delta T/T_c$ for the narrow samples rolled off more slowly as the temperature was lowered. This was a puzzling distinction between the two geometries that we were never able to resolve. Because of this feature, we generally fitted the data for the narrow junctions at temperatures above $0.97T_c$. The resulting values of R_K are generally consistent with those obtained for the wide junctions. Although the 11 values of R_K listed in the table vary by more than a factor of 3, we feel that this is not an unreasonable range given the marked dependence of R_K on the detailed nature of the interfaces with the substrate and the helium bath.

Finally, we comment on the last two columns of Table II. The values of $B(0 \text{ dB})$ inferred from the fits show a very wide range, presumably because of the variability in the coupling of the quartz crystals to the microwave cavity and the aluminum films, and of the strong frequency dependence of the cavity Q and waveguide insertion loss. Thus the ratio of the phonon power incident on the junc-

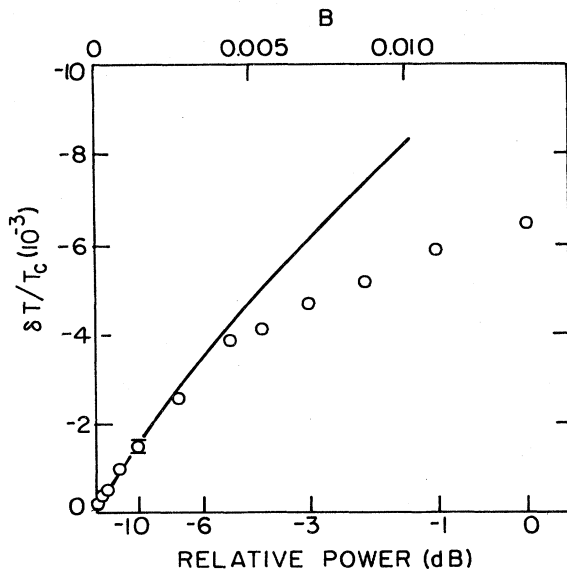


FIG. 9. Gap enhancement vs relative power taken from Fig. 8 at $T/T_c=0.99$. Curve is prediction of Eq. (2.7) from fit at -10 dB .

tion to the microwave power delivered to the waveguide varied enormously from sample to sample. The last column shows the variation in $\delta T/T_c$ measured at 0 dB and at $0.98T_c$. The most noteworthy feature is the fact that the values of $\delta T/T_c$ were generally higher for the narrow junctions than for the wide junctions, a trend for which we have no explanation.

D. Critical-current enhancement

It is clear from Fig. 7 that the critical-current enhancement behaves in a very different way from the gap enhancement. In this section, we investigate whether the

departure of j_c/Δ^3 from its equilibrium value discussed by Entin-Wohlman²⁸ and Weiss²⁷ can account for these differences.

Entin-Wohlman²⁸ showed that in the presence of a nonequilibrium distribution function the supercurrent is related to Δ by a relation of the form

$$j_s \propto \Delta^2 [1 - (4k_B T/\Delta) \delta n(\Delta)], \quad (4.3)$$

where $\delta n(\Delta) \equiv n(\Delta) - n_T(\Delta)$. For phonon irradiation we have, from Eq. (2.2), $\delta n(\Delta) = -B(2\Delta/h\nu + 1)^{-1/2}$. When this effect is included in Eq. (2.9), together with the kinetic energy of the supercurrent,²⁷ Eq. (2.10), one arrives at the equation

$$\frac{T - T_c}{T_c} + \beta \left[\frac{\Delta}{k_B T_c} \right]^2 + \frac{4}{27\beta^2} \left[\frac{k_B T_c}{\Delta} \right]^4 \frac{(j_s/j_{c0})^2}{[1 - (4k_B T/\Delta) \delta n(\Delta)]^2} = B [G(\Delta/h\nu) - (h\nu/k_B T_c)H]. \quad (4.4)$$

One solves this equation self-consistently for the critical current j_c for fixed values of T , ν , B , and H . This value of j_c is used to calculate the theoretical value of $\delta T/T_c$ from

$$T/T_c - 1 + (j_c/j_{c0})^{2/3} = -\delta T/T_c. \quad (4.5)$$

In Fig. 10 we show the computed values of $\delta T/T_c$ vs T/T_c for $h\nu/k_B T_c = 0.333$, $B = 0.01$ and 0.03 , and $H = 1.6$ (chosen to correspond to sample *W4*). The solid line represents the gap enhancement calculated in the usual way with $j_s = 0$, the dotted line represents the critical-current enhancement including the correction for the kinetic energy term only,²⁷ while the dashed line includes corrections for both the kinetic energy and the nonequilibrium distribution. At each power level, we observe that

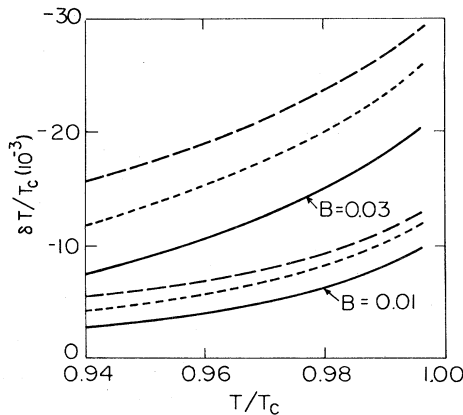


FIG. 10. Computed values of $\delta T/T_c$ vs T/T_c for $h\nu/k_B T_c = 0.333$, $B = 0.01$ and 0.03 , and $H = 1.6$. Solid line is gap enhancement, dotted line is critical-current enhancement with kinetic energy term included, and dashed line is critical-current enhancement with kinetic energy term and nonequilibrium distribution included.

both corrections have the effect of adding a roughly constant value of $\delta T/T_c$ to the gap enhancement curve. For each power level, at $T/T_c = 0.98$ the combined corrections are about 50% of the gap enhancement with $j_s = 0$. Figure 11 shows the power dependence of the enhancements at $T/T_c = 0.99$; the notation is as for Fig. 10. We observe that the difference between the gap and critical-current enhancements is nearly linear in B .

Comparing the results in Fig. 10 with the experimental data in Fig. 7, we see that they are qualitatively different: The experimental values of the critical-current enhancement (in terms of $\delta T/T_c$) remain approximately constant from $0.99T_c$ down to the lowest temperature studied, while the theory predicts a steady decrease over this temperature range. Furthermore, at a given temperature and phonon power the increase in $\delta T/T_c$ predicted for the critical current over that gap is much too small to account for the experimental discrepancies. Thus, although it is obviously necessary to take into account both the kinetic term and the nonequilibrium distribution when one com-

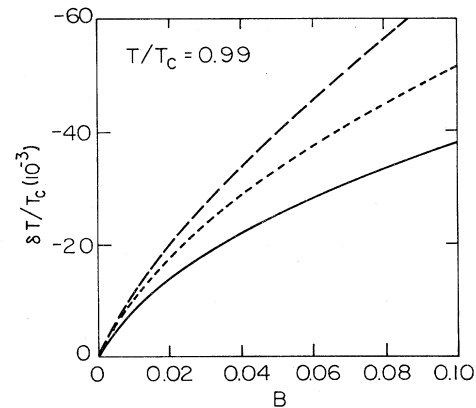


FIG. 11. Computed values of $\delta T/T_c$ vs B at $T/T_c = 0.99$ for $h\nu/k_B T_c = 0.333$ and $H = 1.6$. Notation as in Fig. 10.

putes the critical-current enhancement, we are forced to conclude that these corrections are not able to account for the observed differences between the gap and critical-current enhancements.

E. Linearity of phonon power

Throughout the discussion of our results, we assumed that the phonon power incident on the samples was linearly proportional to the microwave power delivered to the cryostat. To test this assumption, we performed measurements in which the temperature was raised until the test film was in the normal state, while the electrode with the higher transition temperature was still superconducting. We used the low-voltage region of the current-voltage characteristic of the superconducting-insulator-normal junction as a thermometer, by measuring the height of the voltage pulses produced by the phonon pulses when the junction was biased with a constant current. We obtained the rise in temperature ΔT induced by the phonons by comparing the magnitude of the voltage pulses with the temperature dependence of the equilibrium current-voltage characteristic. The measured value of $\Delta T/T_c$ for *W7* is plotted versus the microwave power in Fig. 12; from the measurements below T_c , we estimate that, at T_c , $B(0 \text{ dB})$ was 0.164. We observe that for values of B up to 0.10, $\Delta T/T_c$ is linear in the microwave power, but that at higher power levels, the response becomes nonlinear. Part of this nonlinearity arises because ΔT is sufficiently large that the Kapitza resistance drops significantly. Another likely cause of the nonlinearity is the nonthermal nature of the quasiparticle distribution in the presence of the injected phonons, so that we cannot properly ascribe a temperature to the system. However, since all of our data were fitted at values of B substantially below 0.1, we have confidence that the phonon power is proportional to the microwave power over the range of interest.

V. CONCLUDING SUMMARY

We have performed a detailed investigation of the phonon-induced gap and critical-current enhancements of

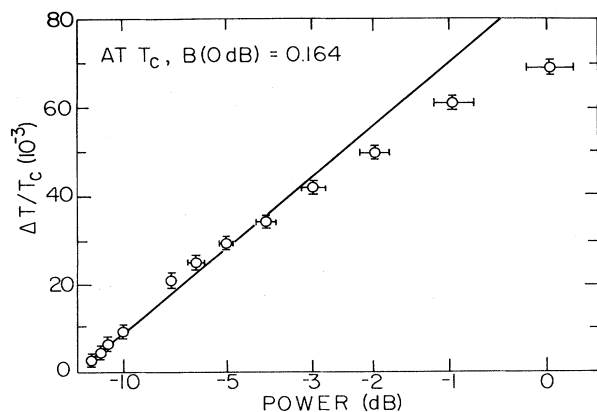


FIG. 12. $\Delta T/T_c$ vs relative power for junction *W7* at $T/T_c = 1.009$. Straight line is fitted to data at low values of B .

superconducting Al films. We studied the gap enhancement with two types of junctions, wide (typically $300 \times 300 \mu\text{m}^2$) and narrow (typically $300 \times 10 \mu\text{m}^2$). The gap enhancements for all of the samples showed the same general features, increasing smoothly with power at fixed temperature and decreasing with decreasing temperature at fixed phonon power, except very close to T_c where the enhancement rolled off as the temperature was increased. However, the gap enhancement decreased less rapidly with decreasing temperature for the narrow junctions than for the wide samples, for reasons we cannot explain.

We fitted the gap enhancement data to the theory²³ for $T/T_c \gtrsim 0.95$ and 0.97 for wide and narrow samples, respectively, and at low phonon power levels to find values of the parameters B and H . Except very close to T_c , where the theory did not predict the observed roll-off in the enhancement, the fit was good. The values of R_K deduced from H were in reasonable agreement with theoretical estimates. At higher levels of phonon power (above a value that varied considerably from sample to sample), the data fell markedly below the predictions of the theory. Our estimates of the parameter τ_{es}/τ_B indicate that it was always less than unity, so that phonon trapping effects should not have affected the data in a major way.^{24,25} Thus the reason for the failure of the theory at the higher power levels is not entirely clear; possibly it reflects a breakdown of the perturbation approach.

The critical-current enhancements were always larger in magnitude (in terms of $\delta T/T_c$) than the gap enhancement. Furthermore, at a fixed phonon power level the critical-current enhancements were nearly independent of temperature except near pair breaking when the enhancements went abruptly to zero. We have calculated the corrections to the equilibrium relation $j_c \propto \Delta^3$ due to the nonequilibrium quasiparticle distribution²⁸ and the kinetic energy of the pairs,²⁷ but found that these contributions were unable to resolve the discrepancy between the gap and critical-current enhancements. Thus we are left with the strong suspicion that there is an additional mechanism responsible for critical-current enhancement, a view consistent with the results of Dahlberg *et al.*,⁸ who observed substantial microwave-induced critical-current enhancement without any discernible gap enhancement.

ACKNOWLEDGMENTS

We are grateful to John Chi for his assistance in the early part of this work, to Robert Wilson for his instruction in the operation of the traveling-wave tube, and to E. L. Hahn and C. H. Townes for the loan of microwave equipment. We are indebted to E. H. Jacobsen, J. E. Mooij, A. Schmid, and G. Schön for helpful discussions. We acknowledge the use of the Microelectronics Facility in the Electronics Research Laboratory of Electrical Engineering and Computer Science Department, University of California, Berkeley. This work was supported by the Director, Office of Energy Research, Office of Basic Energy Sciences, Materials Sciences Division of the U. S. Department of Energy under Contract No. DE-AC03-76SF00098.

- ¹A. F. G. Wyatt, V. M. Dmitriev, W. S. Moore, and F. W. Sheard, *Phys. Rev. Lett.* **16**, 1166 (1966).
- ²A. H. Dayem and J. J. Wiegand, *Phys. Rev.* **155**, 419 (1967).
- ³G. M. Eliashberg, *Zh. Eksp. Teor. Fiz. Pis'ma Red.* **11**, 186 (1970) [*JETP Lett.* **11**, 114 (1970)]; B. I. Ivlev and G. M. Eliashberg, *ibid.* **13**, 464 (1971) [**13**, 33 (1971)]; G. M. Eliashberg, *Zh. Eksp. Teor. Fiz.* **61**, 1254 (1971) [*Sov. Phys.—JETP* **34**, 668 (1972)]; B. I. Ivlev, S. G. Lisitsyn, and G. M. Eliashberg, *J. Low Temp. Phys.* **10**, 449 (1973).
- ⁴Yu. I. Latyshev and F. Ya. Nad', *Zh. Eksp. Teor. Fiz.* **71**, 2158 (1976) [*Sov. Phys.—JETP* **44**, 1136 (1976)].
- ⁵K. W. Shepard, *Physica* **55**, 786 (1971).
- ⁶T. M. Klapwijk, J. N. Van den Bergh, and J. E. Mooij, *J. Low Temp. Phys.* **26**, 385 (1977).
- ⁷J. A. Pals and J. Dobben, *Phys. Rev. B* **20**, 935 (1979).
- ⁸E. D. Dahlberg, R. L. Orbach, and I. K. Schuller, *J. Low Temp. Phys.* **36**, 367 (1979).
- ⁹T. Kammers and J. Clarke, *Phys. Rev. Lett.* **38**, 1091 (1977).
- ¹⁰C. M. Falco, T. R. Werner, and I. K. Schuller, *Solid State Commun.* **34**, 585 (1980).
- ¹¹J. E. Mooij, N. Lambert, and T. M. Klapwijk, *Solid State Commun.* **36**, 535 (1980).
- ¹²J. T. Hall, L. B. Holdeman, and R. J. Soulen, Jr., *Phys. Rev. Lett.* **45**, 1011 (1980).
- ¹³L. B. Holdeman, J. T. Hall, D. van Vechten, and R. J. Soulen, Jr., *Physica* **108B**, 827 (1981).
- ¹⁴R. E. Horstman and J. Wolter, *Phys. Lett.* **82A**, 43 (1981).
- ¹⁵J. A. Pals and J. Dobben, *Phys. Rev. Lett.* **44**, 1143 (1980).
- ¹⁶P. M. Th. M. van Attekum and J. J. Ramekers, *Solid State Commun.* **43**, 735 (1982).
- ¹⁷P. M. Th. M. van Attekum, J. J. Ramekers, J. A. Pals, and A. A. M. Hoeben, *Phys. Rev. B* **27**, 1623 (1983).
- ¹⁸T. J. Tredwell and E. H. Jacobsen, *Phys. Rev. Lett.* **33**, 244 (1975); *Phys. Rev. B* **13**, 2931 (1976).
- ¹⁹K. E. Gray, *Solid State Commun.* **23**, 633 (1978).
- ²⁰C. C. Chi and J. Clarke, *Phys. Rev. B* **20**, 4465 (1979).
- ²¹J. E. Mooij, in *Nonequilibrium Superconductivity, Phonons and Kapitza Boundaries*, edited by K. E. Gray (Plenum, New York, 1981).
- ²²J. A. Pals, K. Weiss, P. M. T. M. van Attekum, R. E. Horstman, and J. Wolter, *Phys. Rep.* **89**, 323 (1982).
- ²³U. Eckern, A. Schmid, M. Schmutz, and G. Schön, *J. Low Temp. Phys.* **36**, 643 (1979).
- ²⁴J. J. Chang and D. J. Scalapino, *J. Low Temp. Phys.* **29**, 477 (1977).
- ²⁵N. C. Cirillo, W. L. Clinton, and J. R. Waterman, *Phys. Rev. B* **25**, 5698 (1982).
- ²⁶P. Lesieur and N. Perrin, *J. Low Temp. Phys.* **50**, 545 (1983).
- ²⁷K. Weiss, *Phys. Lett.* **82A**, 423 (1981).
- ²⁸O. Entin-Wohlman, *J. Low Temp. Phys.* **43**, 91 (1981).
- ²⁹J. E. Mooij and T. M. Klapwijk, *Phys. Rev. B* **27**, 3054 (1983).
- ³⁰Michael Tinkham, *Introduction to Superconductivity* (McGraw-Hill, New York, 1975).
- ³¹W. J. Skocpol, *Phys. Rev. B* **14**, 1045 (1976).
- ³²N. W. Ashcroft and N. D. Mermin, *Solid State Physics* (Holt, Rinehart, and Winston, New York, 1976).
- ³³K. A. Gschneidner, *Solid State Phys.* **16**, 275 (1964).
- ³⁴T. R. Lemberger and J. Clarke, *Phys. Rev. B* **23**, 275 (1981).
- ³⁵R. Meservey and B. B. Schwartz, in *Superconductivity*, edited by R. D. Parks (Marcel Dekker, New York, 1969), p. 174.
- ³⁶S. B. Kaplan, *J. Low Temp. Phys.* **37**, 343 (1979).
- ³⁷F. R. Fickett, *Cryogenics* **11**, 349 (1971).
- ³⁸C. C. Chi and J. Clarke, *Phys. Rev. B* **19**, 4495 (1979).
- ³⁹A. B. Pippard, *Philos. Mag.* **46**, 1104 (1955).
- ⁴⁰With 9-GHz phonons, a film thickness of 100 nm, and a film resistivity $\rho = 20$ n Ω m, the standard theory of ultrasonic attenuation (Ref. 39) predicts that 0.15% of the incident power is absorbed for a single pass of the phonons through the film.
- ⁴¹O. Entin-Wohlman, *Phys. Rev. B* **22**, 5225 (1980).
- ⁴²R. E. Horstman, J. Wolter, and E. J. Bartels, *Physica* **108B**, 833 (1981).
- ⁴³L. Solymar, *Superconducting Tunneling and Applications* (Wiley-Interscience, New York, 1972).
- ⁴⁴Throughout this paper, we quote the value of R_K at T_c ; values in the literature are often quoted for 1 K.
- ⁴⁵A. C. Anderson, in *Nonequilibrium Superconductivity, Phonons and Kapitza Boundaries*, edited by K. E. Gray (Plenum, New York, 1981).
- ⁴⁶A. F. G. Wyatt, in *Nonequilibrium Superconductivity, Phonons and Kapitza Boundaries*, edited by K. E. Gray (Plenum, New York, 1981).
- ⁴⁷We have used the value obtained by J. T. Follinsbee and A. C. Anderson [*Phys. Rev. Lett.* **31**, 1580 (1973)] for the Cu/He interface. The values of the Kapitza resistance between He⁴ and a large number of solids are spread over only a factor of 3 (Ref. 48) unless the interfaces are extraordinarily clean.
- ⁴⁸O. V. Lounasmaa, *Experimental Principles and Methods below 1 K* (Academic, New York, 1974).
- ⁴⁹J. D. N. Cheeke, H. Ettinger, and B. Hebral, *Can. J. Phys.* **54**, 1749 (1976).
- ⁵⁰V. E. Holt, *J. Appl. Phys.* **37**, 798 (1966).
- ⁵¹S. B. Kaplan, C. C. Chi, D. N. Langenberg, J. J. Chang, S. Jafarey, and D. J. Scalapino, *Phys. Rev. B* **14**, 4854 (1976).